

PAPER • OPEN ACCESS

The use of multiconductor strip structures for splitting an ultrashort pulse in its generation systems

To cite this article: A O Belousov *et al* 2019 *J. Phys.: Conf. Ser.* **1399** 022049

View the [article online](#) for updates and enhancements.



IOP | ebooks™

Bringing you innovative digital publishing with leading voices to create your essential collection of books in STEM research.

Start exploring the collection - download the first chapter of every title for free.

The use of multiconductor strip structures for splitting an ultrashort pulse in its generation systems

A O Belousov^{1,2}, I V Romanchenko² and T R Gazizov¹

¹ Tomsk State University of Control Systems and Radioelectronics, 40, Lenina ave., Tomsk, 634050, Russia

² Institute of High Current Electronics, Siberian Branch, Russian Academy of Sciences, 2/3 Akademicheskoy ave., Tomsk, 634055, Russia

E-mail: ant1lafleur@gmail.com

Abstract. The article explores the ways to use multiconductor strip lines (SL) for solving the problems of generating a bipolar and unipolar pulse oscillations packet. Reflection-symmetric and five-conductor microstrip structures, as well as their various configurations, which are cascade-connections of these SLs are considered. The maximum conversion efficiency of a unipolar nanosecond pulse into high-frequency oscillations is estimated to be less than 1–2%. The results are important for further research and the possibility of using SLs for such tasks.

1. Introduction

Currently, the task of generating powerful microwave pulses is becoming especially urgent due to the increasingly recognized need to counter robotic systems, especially unmanned aerial vehicles [1]. It seems that over time, the threat emanating from such complexes will only increase, which makes the research and development in the field of electromagnetic counteraction highly relevant [2].

Meanwhile, narrow-band devices based on the use of a relativistic electron beam, as well as ultra-wide-band (UWB) generators based on semiconductor switches, can be distinguished among the highly-sought sources of high-power microwave pulses [3–5]. These two classes of generators, despite their advantages, also have certain disadvantages: relativistic devices are quite large-sized, and solid-state UWB generators, though having a small size, emit relatively small amount of energy. Therefore, the search for a new approach to creating sources of high-power microwave pulses, which would combine the compactness of solid-state generators and high radiated energy achieved through the use of multiple solid-state elements in one device, in contrast to UWB generators, where single sharpeners are used, is a relevant task. The approach in which the microwave power generated in periodically arranged sharpeners is distributed between a certain number of oscillations (>10) due to artificial dispersion in the transmission line is of particular interest [6]. Typically, this approach considers two-conductor transmission lines. This article analyzes the propagation of a nanosecond pulse with a short front along multiconductor strip lines (SL), the structure of which allows you to distribute the pulse energy along the transmission line, forming an oscillatory waveform.

2. Structures and circuits under investigation

For simulation, we chose multiconductor SLs consisting of 4–5 conductors. Their detailed research, as well as a full-scale experiment in the time domain, is performed in [7, 8]. First, we constructed



geometric models of the SL cross-section. Then, we calculated the matrixes of per-unit-length coefficients of electrostatic \mathbf{C} and electromagnetic \mathbf{L} induction. To account the losses, we calculated the matrixes of the per-unit-length resistances \mathbf{R} (for the losses in the conductors) and conductivities \mathbf{G} (for the losses in the dielectrics). To calculate the elements of the \mathbf{G} -matrix we used a widely known model [9] of the relative permittivity frequency dependence and the tangent of the dielectric loss angle of the dielectric material FR-4. The entries of the \mathbf{R} -matrix were calculated taking into account the skin effect, the proximity effect and losses in the ground plane using the method proposed in [10]. Next, we drew a schematic diagram for simulation, set loads and pulse excitation values, and computed time response to the excitation in the parameter range.

The cross-sections of these lines are generally shown in Figure 1, where w is the width of conductors, s_i is separations between them, t is the thickness of conductors, h is the thickness of the dielectric and ϵ_r is the permittivity of the dielectric.

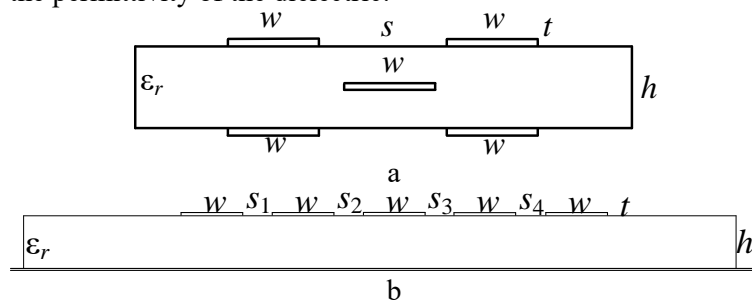


Figure 1. Cross-sections of reflection-symmetric (a) and five-conductor microstrip (b) structures.

The schematic diagrams of these SLs are shown in Figure 2. In the simulation of single segments of reflection-symmetric and five-conductor structures, the resistance values (R_G , R_L and R) were taken equal to 50Ω with a length (l) of 1 m.

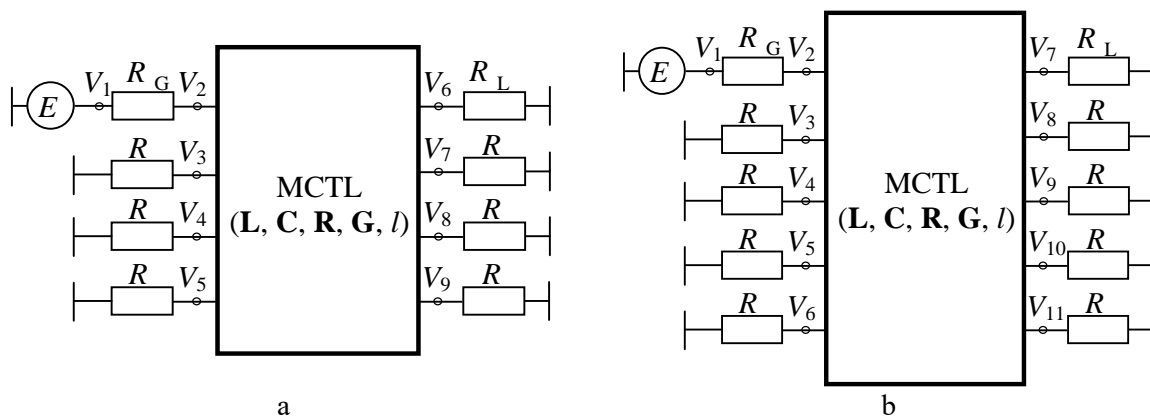


Figure 2. Schematic diagrams of reflection-symmetric (a) and five-conductor microstrip (b) structures.

It was assumed that a T-wave was propagating along the considered SLs. The parameters and waveforms of the SLs were calculated in the TALGAT software product [11, 12] that provides acceptable accuracy, does not require high computational costs, and implements the above models and steps.

As an excitation pulse, we used a trapezoidal pulse with rise, fall and flat top durations of 1 ns (total duration 3 ns, to approximate a typical ultrashort pulse (USP)) with an amplitude of 100 V (measured at a load of 50Ω). Since the article considers not only the formation of a bipolar pulse oscillations packet but also of unipolar ones, these SLs are considered not only as a single form, but also in various cascade connections. The following cases of cascading were considered: 3 cascaded

segments of a reflection-symmetric structure (configuration 1); 3 cascaded segments of a five-conductor structure with an active outer conductor (configuration 2); 3 cascaded segments of a five-conductor structure with an active central conductor (configuration 3); 3 cascaded segments of a five-conductor structure with 2 active outer conductors (configuration 4) and 4 cascaded segments of a five-conductor structure (configuration 5). It is known that when SLs made of N conductors is cascade-connected, each pulse is sequentially divided into N pulses of smaller amplitude. These pulses will not coincide with each other in time if the difference in mode delays for each subsequent segment is at least twice as large as for the previous one. Thus, the cascade-connected SLs of N conductors will, under certain conditions, lead to a decomposition into 2^N pulses, which is possible with sequential doubling or shortening of the cascaded segments lengths [13]. Therefore, in cascading configurations 1–4, l of each next segment is twice as large as the previous one, so $l_1=0.2$ m, $l_2=0.4$ m and $l_3=0.8$ m, so $l_2=1.4$ m. Due to the specificity of cascading configuration 5, the lengths of the segments are taken equal to $l_1=0.4$ m, $l_2=0.4$ m, $l_3=0.4$ m and $l_4=0.8$ m, so $l_2=2$ m.

3. Simulation results

This section presents the main simulation results of various SLs. To form a bipolar pulse oscillations packet, the open-circuit mode was set at the ends of passive conductors by setting the resistance values (R) to 10 k Ω . Schematic diagrams of the investigated structures are presented in Figure 2. The cascade connections of configurations 1–5 were also investigated.

During the formation of a unipolar pulse oscillations packet, the resistance symmetry was ensured by setting their values (R_G , R_L and R) equal to 50 Ω . Note that only the voltage from the $V/2$ node goes to the SL (Figure 2). The amplitude of this voltage directly depends on the SL matching with the path, and it is with respect to this value that the pulse attenuation by the protective devices included in the circuit is estimated. At this stage of the study, the ideal SL matching (both single and cascaded) with the path was not observed. Schematic diagrams of the structures under investigation are presented in Figure 2; the schematic diagram of a five-conductor line with an active central conductor and cascade connection of configurations 1–3 were also investigated.

3.1. The formation of a bipolar pulse oscillations packet in multiconductor SLs

The simulation was performed at the following cross-section values of the reflection-symmetric structure: $s=200$ μm , $w=1800$ μm , $t=18$ μm , $h=500$ μm and $\epsilon_r=4,5$. In the five-conductor, only the width of the conductors differed ($w_i=1000$ μm). Figures 3–5 show the voltage waveforms obtained by simulating various SLs.

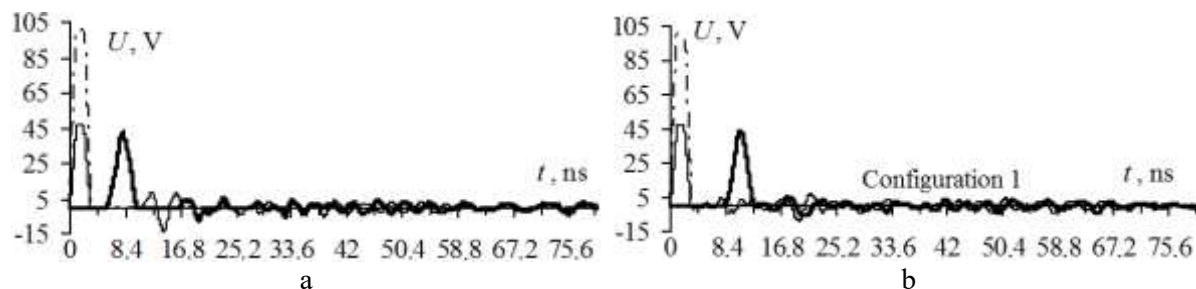


Figure 3. Voltage waveforms of EMF (---), the signal at the input (—) and output (—) of the reflection-symmetric line (a) and 3 cascaded segments of the reflection-symmetric structure (b).

Based on the obtained dependences, the maximum energy efficiency of pulse formation in the form of pulse oscillations packet (the ratio of the energy of the output and input pulses) was calculated for two cases: the output signal with taking into account the main pulse that arrived at the end of the SL (which contains the largest amount of energy), and the one without it. For the reflection-symmetric line it was 71.12% and 2.7%, configuration 1 – 87.63% and 8.38%, the five-conductor line – 87.2% and 1.3%, configuration 2 – 92.2% and 2.89%, configuration 3 – 93.3% and 5.7%, configuration 4 –

94.2% and 4.5%, as well as 94.23% and 4.49% (since there are 2 active outer conductors in this configuration) and configuration 5 – 47.6% and 6.8%.

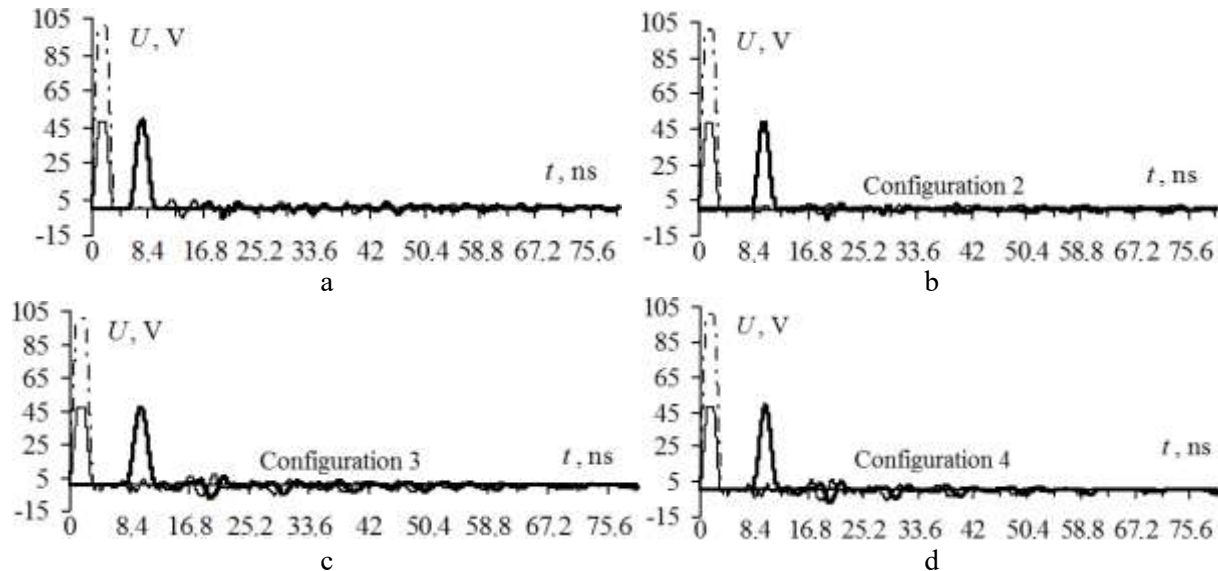


Figure 4. Voltage waveforms of EMF (---), the signal at the input (—) and output (—) of the five-conductor line (a), 3 cascaded segments of the five-conductor structure with an active outer conductor (b), 3 cascaded segments of the five-conductor structure with an active central conductor (c) and 3 cascaded segments of the five-conductor structure with 2 active outer conductors (d).

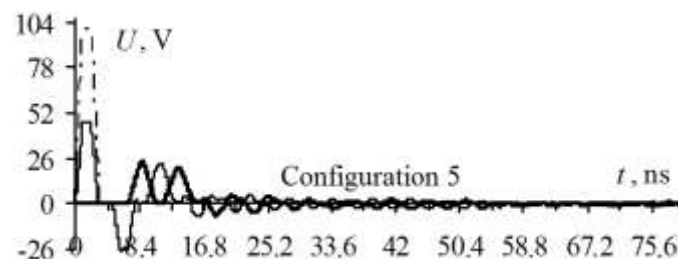


Figure 5. Voltage waveforms of EMF (---), the signal at the input (—) and output (—) of 4 cascaded segments of the five-conductor structure.

Obviously, the most apparent level of the bipolar pulse oscillations packet, as well as the highest conversion efficiency (without the main pulse that came to the end of the SL), is achieved by simulating the reflection-symmetric cascade-connection structure (configuration 1) and amounts to 8.38%. An acceptable result is also observed when simulating configuration 5, which consists of 4 cascaded segments of the five-conductor structure.

The best conversion efficiency level (configuration 1) was probably obtained due to the symmetry of the SL cross-section. In addition, an acceptable level of conversion efficiency (configuration 5) was obviously obtained due to the decomposition of the input pulse (node V_2) into two pulses at the end of the structure (in the other structures and configurations the decomposition was not observed), which were subsequently induced on passive conductors due to the strong coupling, and underwent reflections from resistances, thereby forming a bipolar pulse oscillations packet. Meanwhile, in the remaining configurations of five-conductor structures, the conversion efficiency does not exceed 5.7% (configuration 3).

It should be noted that the oscillations are non-harmonic and in some cases non-periodic in nature, and also contain a fraction of the near zero frequency energy. Thus, from the point of view of

generating radiated emissions, the efficiency of converting a nanosecond pulse into radiated emissions will be no more than 1–2%, which is associated, among others, with large losses in the SL.

3.2. *The formation of a unipolar pulse oscillations packet in multiconductor SLs*

The simulation was performed at the following cross-section values of the reflection-symmetric structure: $s=450\ \mu\text{m}$, $w=2000\ \mu\text{m}$, $t=18\ \mu\text{m}$, $h=500\ \mu\text{m}$ and $\epsilon_r=20$; the five-conductor structure with an active outer conductor: $s_1=10\ \mu\text{m}$, $s_2=50\ \mu\text{m}$, $s_3=200\ \mu\text{m}$, $s_4=850\ \mu\text{m}$, $w_i=1000\ \mu\text{m}$, $t=35\ \mu\text{m}$, $h=500\ \mu\text{m}$, $\epsilon_r=20$; and the five-conductor structure with an active central conductor: $s_1=200\ \mu\text{m}$, $s_2=100\ \mu\text{m}$, $s_3=10\ \mu\text{m}$, $s_4=100\ \mu\text{m}$, $w_i=1000\ \mu\text{m}$, $t=35\ \mu\text{m}$, $h=500\ \mu\text{m}$ and $\epsilon_r=20$. When simulating the time response of single segments of the reflection-symmetric structure, the five-conductor structure with an active outer conductor, and the five-conductor structure with an active central conductor, the trapezoidal pulse with rise, fall and flat top durations of 50 ps (total duration 150 ps) with an amplitude of 100 V was used as an excitation. Figures 6 and 7 show the voltage waveforms obtained by simulating the following structures: the reflection-symmetric structure, the five-conductor structure with an active outer conductor and the five-conductor structure with an active central conductor, as well as configurations 1–3.

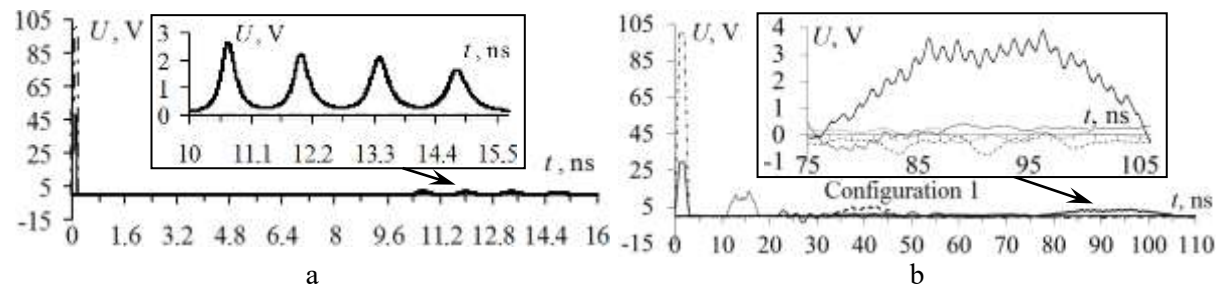


Figure 6. Voltage waveforms of EMF (---), the signal at the input (—) and output (—) of the reflection-symmetric line (a) and 3 cascaded segments of the reflection-symmetric structure (b).

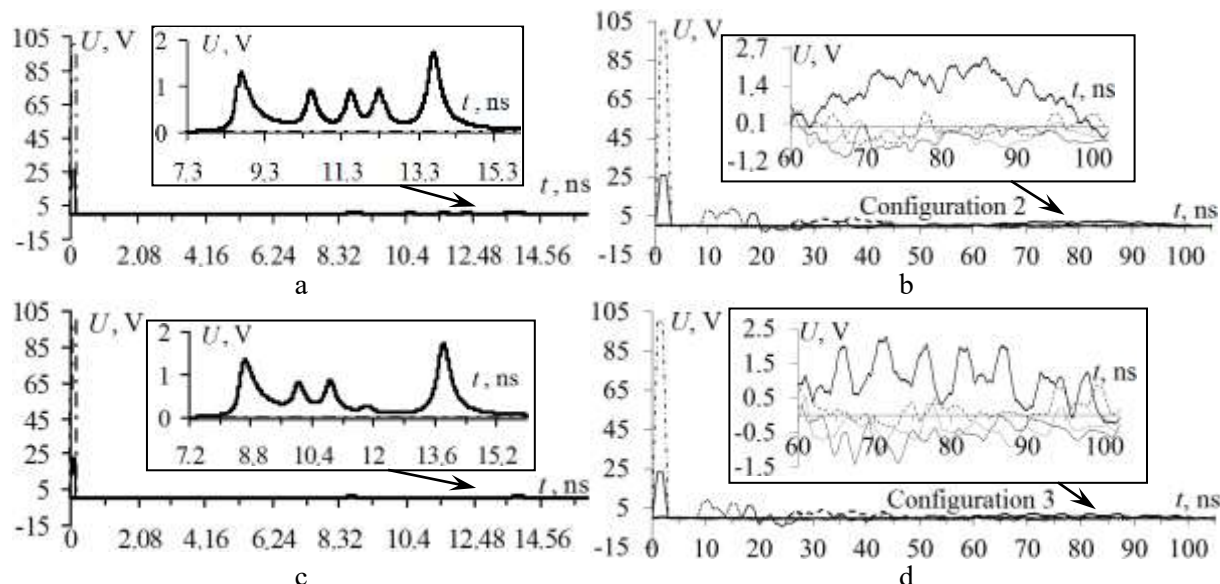


Figure 7. Voltage waveforms of EMF (---), the signal at the input (—) and output (—) of the five-conductor structure with an active outer conductor (a), 3 cascaded segments of the five-conductor structure with an active outer conductor (b), the five-conductor structure with an active central conductor (c) and 3 cascaded segments of the five-conductor structure with an active central conductor (d).

Based on the obtained dependences, we also calculated the maximum conversion efficiency of the pulse oscillations packet for the voltage waveforms obtained with the cascade connection of the SL. For configuration 1, it was 16.6%, configuration 2 – 12.1%, configuration 3 – 11.9%.

The formation of a unipolar pulse oscillations packet in the SL was achieved using the modal filtering effect [2]. However, there are some differences: modal filtering assumes a complete decomposition of the excitation into the pulse sequence in which the total pulse duration is less than the modulus of the propagating mode delay difference in the SL, whereas this condition was not completely satisfied when the unipolar pulse oscillations packet was formed. In addition, the shape of the output voltage is influenced by dispersion and losses in the conductors and dielectric, which leads to the front and drop «roll-off» of each output pulse, i.e. partial overlap occurs, which forms the unipolar pulse oscillations packet.

We note that configuration 1 is the most optimal (Figure 6 b), since it provides not only the maximum energy conversion efficiency (16.6%), but also a periodic nature of the oscillations. However, from the point of view of generating radiation, high-pass filtering is required, after which the efficiency of converting a nanosecond pulse into radiation will be about 1–2%.

4. Conclusion

Thus, the paper presents the results of research into the use of multiconductor SLs for the problems of forming bipolar and unipolar pulse oscillations packet. The influence of line losses during simulation leads to a decrease in the amplitude of the decomposition pulses and an increase in their duration due to dispersion. In this case, the energy at the output of the multiconductor lines is 8–16% of the input pulse energy, and the efficiency of conversion into a useful oscillating signal, which can be emitted by an antenna with a sufficiently wide band, does not exceed 1–2%. It should be noted here that there are no nonlinear elements in the lines that enrich the spectrum of the pulse with a high-frequency component. However, the presence of significant losses in the line suggests that the addition of nonlinear sharpening elements to the line will not significantly increase the efficiency in the proposed configurations of multiconductor SLs.

Acknowledgments

The reported study was funded by the Ministry of Science and Higher Education of the Russian Federation (Projects 8.9562.2017/8.9 and 0291-2019-0001).

References

- [1] Semenets V O and Trukhin M P 2018 *H&ES Research* **10(3)** 4–12
- [2] Makarenko S I 2016 *Systems of Control, Communication and Security* **2** 73–132
- [3] Belichenko V P, Buyanov Yu I and Koshelev V I 2015 *Novosibirsk: Science* **473**
- [4] Benford J, Swegle J A and Schamiloglu E 2007 *Wiley – IEEE Press* **531**
- [5] Ulmaskulov M R, Pedos M S, Rukin S N, Sharypov K A, Shpak V G, Shunailov S A, Yalandin M I, Romanchenko I V and Rostov V V 2015 *Review of Scientific Instruments* **86** 074702
- [6] Belyantsev A M, Dubnev A I, Klimin S L *et al.* 1995 *Technical Physics* **65** 132–42
- [7] Belousov A O and Gazizov T R 2018 *Complexity* **2018** 1–15
- [8] Zhechev Y S, Chernikova E B, Belousov A O and Gazizov T R 2019 *Systems of Control, Communication and Security* **2** 162–79
- [9] Djordjevich A R, Biljic R M, Likar-Smiljanic V D and Sarkar T K 2001 *IEEE Transactions on Electromagnetic Compatibility* **43(4)** 662–6
- [10] Matthaie G L and Chinn G C 1992 *Microwave Symposium Digest* 1353–4
- [11] Orlov P E and Buichkin E N *18th International conference on micro/nanotechnologies and electron devices* 54–8
- [12] Kuksenko S P 2019 *IOP Conf. Series: Materials Science and Engineering* **560** 1–7
- [13] Gazizov T, Melkozerov A, Zabolotsky A, Kuksenko S, Orlov P, Salov V, Akhunov R,

Kalimulin I, Surovtsev R, Komnatnov M and Gazizov A 2015 *Proceedings of the International conference on Applied Physics, Simulation and Computers* pp 151–62